Agour, Mostafa ; Falldorf, Claas ; Bergmann, Ralf B.

Fast form measurements using a digital micro-mirror device in imaging with partially coherent illumination

Journal Article as: peer-reviewed accepted version (Postprint)

DOI of this document*(secondary publication): https://doi.org/10.26092/elib/3818

Publication date of this document: 16/04/2025

* for better findability or for reliable citation

Recommended Citation (primary publication/Version of Record) incl. DOI:

Mostafa Agour, Claas Falldorf, and Ralf B. Bergmann, "Fast form measurements using a digital micro-mirror device in imaging with partially coherent illumination," Opt. Lett. 45, 6154-6157 (2020).
DOI: https://doi.org/10.1364/OL.411106

Fast form measurements using a digital micro-mirror device in imaging with partially coherent illumination

Mostafa Agour,[1,2,*] **Claas Falldorf,**[1] **and Ralf B. Bergmann**[1,3]

[1] BIAS—Bremer Institut für angewandte Strahltechnik, Klagenfurter Str. 5, 28359 Bremen, Germany
[2] Aswan University, Faculty of Science, Department of Physics, Aswan 81528, Egypt
[3] University of Bremen, Faculty 01: Physics and Electrical Engineering and MAPEX Center for Materials and Processes, 28359 Bremen, Germany
*Corresponding author: agour@bias.de

Received 30 September 2020; revised 19 October 2020; accepted 19 October 2020; posted 19 October 2020 (Doc. ID 411106); published 9 November 2020

We present a new technique for fast form measurement based on imaging with partially coherent illumination. It consists of a $4f$-imaging system with a digital micro-mirror device (DMD) located in the Fourier plane of its two lenses. The setup benefits from spatially partially coherent illumination that allows for depth discrimination and a DMD that enables a fast depth scan. Evaluating the intensity contrast, the 3D form of an object is reconstructed. We show that the technique additionally offers extended depth of focus imaging in microscopy and short measurement times of less than a second.

Quality assurance during the fabrication of microscopic technical objects, e.g., parts from deep drawing, is an essential requirement within production. Parts have to be tightly toleranced since they are the basis for large assemblies. In addition, mass production requires rapid measurement of the 3D geometry of micro parts. However, due to industrial requirements, the measurement technique should also be robust against mechanical distortions [1]. Due to its non-contact and non-invasive properties, optical metrology techniques can offer all of these properties.

While optical tactile and confocal microscopy approaches are too slow, interferometric methods such as digital holography [2] and white light interferometry [3] or coherence radar [4] have been established for full field measurement. However, the result of the measurement is prone to environmental disturbances such as vibrations or thermal fluctuations, since the interfering wave fields travel along separated paths. In this work, we will show that in the case of spatially partially coherent illumination, the 3D shape of an object is encoded into the spatial coherence function by a simple depth scanning speckle imaging process. In contrast to the aforementioned interferometric techniques, speckle imaging is a common path process and therefore has low demands regarding mechanical stability. Additionally, the limited spatial coherence is achieved by an extended light source. In our experiments we achieved depth scanning at kilohertz rates by means of a digital micro-mirror device (DMD) [5], which results in a short measurement time of less than a second. Thus, no mechanically shifting parts are required within the (vertical) depth scan, in contrast to focus variation techniques [6], for example. Yet, since the method shares similarities with focus variation, it can also provide an extended depth of focus image.

Figure 1 shows a scheme of the proposed system. It is based on a telecentric $4f$-imaging system with a DMD located at the common Fourier plane of two identical lenses with focal length f, which enables amplitude modulation.

In analogy to phase retrieval based on a liquid crystal spatial light modulator (SLM) [7], the DMD is used to modulate the light with the transfer function (TF) of propagation:

$$H_z(\vec{\xi}) = \exp\left[ikz\sqrt{1-\lambda^2|\vec{\xi}|^2}\right], \quad \textbf{(1)}$$

with wave number k, wavelength λ, propagation distance z, and vector $\vec{\xi}$ at the frequency domain. However, since the DMD is an amplitude-only modulator, we have to find a binarized amplitude representation of the TF, which will be discussed in detail below. Since the DMD has switching times in the kilohertz range, rapid propagation scans across different object planes can be realized with this arrangement [5].

We use coherent monochromatic light, which illuminates a rotating diffuser, as shown in Fig. 1. The spatial coherence of the illumination can then be adjusted by altering the spot size r_s across the diffuser's surface. The object has an optically rough surface and is located at a distance of d from the rotating diffuser. If $d \gg r_s$ holds, we can describe the illumination by a set of N mutually independent plane waves, each with a wave vector of $\vec{k}_n$. We are now interested in the speckle image contrast across the sensor plane, which is the primary criterion of our method for focus plane separation.

In this situation, we may refer to a model that predicts the contrast of propagated speckle images under requirements spatially partially coherent illumination [8]. However, here we present a new measurement principle based on speckle contrast. The main novelty of the work is to (i) define the requirements

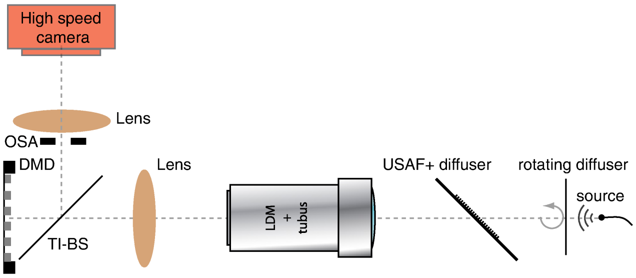

Fig. 1. Schematic of the $4f$ system that employs a digital-mirror device (DMD) located at its common Fourier plane. The test object, a United States Air Force resolution target and a diffuser (USAF + diffuser), is illuminated by a spatially partially coherent light obtained by illuminating a rotating diffuser with light emitted from a He–Ne laser. The diffuser is used to generate a speckle field, while the USAF chart is used to easily visualize in-focus and out-focus. The setup employs a long distance microscope objective and its associated tubus (LDM + tubus) and a total internal reflection beam splitter (TI-BS). The order sorting aperture (OSA) is used to block high diffraction orders letting only the zeroth, +1, and −1 orders pass.

to realize depth discrimination and (ii) develop the corresponding 3D form reconstruction scheme. Let us assume that the variations in $\vec{k}_n$ are small against the aperture of the imaging system. This basically constitutes a paraxial approximation for the illuminating plane waves, which is valid in our case because $d \gg r_s$ holds. A major finding of Ref. [8] is that each of the independent plane waves $\vec{k}_n$ creates the same elementary speckle pattern $I_0(\vec{x}, z)$, which is expressed in the sensor plane as

$$I(\vec{x}, z) = \sum_{n=1}^{N} I_0(\vec{x} + \Delta\vec{x}_n, z). \tag{2}$$

In the focal plane ($z = 0$), all of these identical speckle patterns coincide and form an image with full contrast. However, when the fields propagate further ($z > 0$), they shift laterally by $\Delta\vec{x}_n$, depending on the direction of the plane waves $\vec{e}_{\perp,n}$, i.e.,

$$\Delta\vec{x}_n = z \cdot \vec{e}_{\perp,n}, \tag{3}$$

where $\vec{e}_{\perp,n} = (k_x, k_y)^T/k$ are the lateral (in-plane) components of the illumination directions. We can interpret Eq. (2) as follows: at every point $\vec{x}$ in the sensor plane, the intensity is defined by the average intensity across an area with radius $\Delta\vec{x}_{n,\max}$, which is the maximum shift.

To estimate the impact of this relationship on the contrast, we have to consider the correlation length, i.e., speckle size, of the intensity in the sensor plane. For a limited circular aperture with a diameter D at the DMD plane the correlation length is defined by the radius of the first root of an Airy disc δx [9]:

$$\delta x = 1.22\frac{\lambda f}{D}. \tag{4}$$

As discussed in Ref. [8], the contrast of the intensity $I(\vec{x}, z)$ depends on the ratio β of the averaging radius $\Delta\vec{x}_{\max}$ to the radius of the correlation area δx. Thus, $\beta = \Delta\vec{x}_{\max}/\delta x$ and takes values between zero and one. If $\beta = 0$, which is obtained when $\Delta\vec{x}_{\max} = 0$, i.e., in the focal plane $z = 0$ [see Eq. (3)], all speckle fields generated by the different sources are identical. Accordingly, the contrast is at maximum. However, $\Delta\vec{x}_{\max}$ increases by increasing z. Thus, the contrast decreases and arrives at its minimum when the intensity is averaged over the entire correlation area, i.e., where (in contrast to Ref. [8]) $\Delta\vec{x}_{\max} \geq \delta x$. Thus, one can discriminate between object points located at the input plane of the $4f$ system, $z = 0$, which have maximum contrast, and other points located at $z > 0$ or $z < 0$, which have lower contrast. Considering the limit $\Delta\vec{x}_{\max} = \delta x$ and using Eqs. (3) and (4), the contrast will reach its minimum at a distance z_0 of

$$z_0 \approx 2d\frac{\delta x}{r_s} \quad \text{or} \quad z_0 \approx \frac{r_c}{\mathrm{NA}_{\mathrm{img}}}, \tag{5}$$

based on the spatial coherence length ($r_c = 1.22\lambda d/r_s$) of the illumination and numerical aperture ($\mathrm{NA}_{\mathrm{img}} = D/2f$) of the imaging system. Here we inserted $\Delta\vec{x}_{\max}$ using the angular diameter of the illumination $\phi_{\max} = r_s/2d$ and thus $\Delta\vec{x}_{\max} = zr_s/2d$. Please note that Eq. (5) gives the resolution of the axial scan, which depends on r_c and $\mathrm{NA}_{\mathrm{img}}$.

In our setup, we use the DMD to create different propagation states z of the speckle fields. Yet, the DMD is an amplitude-only modulator and cannot modulate incoming light with a pure phase function, such as the TF of propagation H_z [see Eq. (1)]. In the following, we will therefore find a binarized amplitude-only representation of H_z, and describe the consequences of this approach towards both the setup and the measurement and evaluation process. The transformation is performed in three steps. In the first step, we consider only the real part $H_{\mathrm{Re},z}$ of $H_z = H_{\mathrm{Re},z} + iH_{\mathrm{Im},z}$. The real part is an amplitude-only modulation creating an additional conjugate −1 order, which would not be present with pure phase modulation. In the second step, we use $H_{\mathrm{Re},z}$ to create the amplitude modulation function $M_A = 1 + H_{\mathrm{Re},z}$, which is required to avoid negative values that cannot be generated by an amplitude modulator. However, M_A will also let arise a zeroth order. In the last step, we have to finally binarize M_A by setting all values above one to one, and all values less than or equal to one to zero. The result of that process produces a distribution that looks like Fresnel zone plates. Modulation of the light with the binarized representation $\bar{M}_A$ will form a multitude of higher diffraction orders, with most of the energy centered around −1, zeroth, and +1 orders.

For the measurement process, we are interested only in the +1 order of the modulated light, so we developed a strategy to filter all of the additional orders. Higher orders, from ±2 on, are largely separated and can therefore be filtered by an order stopping aperture (OSA) in the setup, as seen in Fig. 1. However, this approach does not work for the central orders < ±2. They are so close to each other that considerable amounts of energy will pass the OSA, thus disturbing the image formation.

To compensate for the −1 and zeroth orders, we will have a look at the image formation process in the sensor plane. The intensity is given by

$$I_S = (U_0 + U_{+1} + U_{-1}) \cdot (U_0 + U_{+1} + U_{-1})^*$$

$$= \sum_{n=-1}^{1} |U_n|^2 + \sum_{n \neq m} U_n \cdot U_m^*, \tag{6}$$

where U_n denotes the complex amplitude of the nth order. We are particularly interested in the term $|U_{+1}|^2 = I_{+1}$, which represents the propagated image. It is important to understand

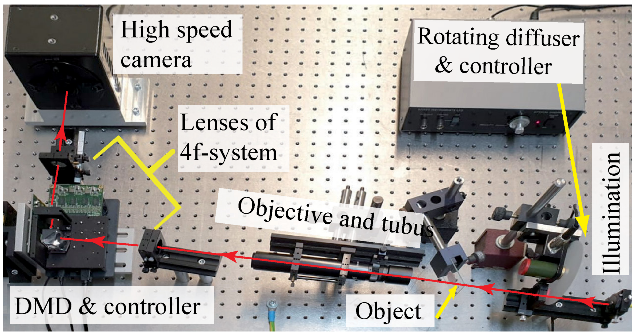

Fig. 2. Experimental setup based on scheme shown in Fig. 1. The red line imitates the propagation of light rays.

the structure of all U_n. The zero-order U_0 is static; we cannot manipulate or change it using the DMD. The term U_{+1} is the complex amplitude of the image in focus, while U_{-1} is the wave field that has been modulated by the complex conjugate of H_z, and therefore represents the out-of-focus image.

We will use the fact that U_{+1} and U_{-1} are in different propagation states. If the setup is arranged in a way z has to be substantially different from zero for U_{+1} to form a focused image of the object, the corresponding U_{-1} will be vastly out of focus. In accord with geometrical optics, the correlation length of each position of U_{-1} becomes approx. 75 time larger than U_{+1}. Thus, the intensity contributions of U_{-1} are approx. 1%. In this case, all terms that contain U_{-1} are negligible. In this situation, Eq. (6) can be approximated to

$$I_S \approx |U_0|^2 + |U_{+1}|^2 + U_0 \cdot U_{+1}^* + U_0^* \cdot U_{+1}. \quad \textbf{(7)}$$

To isolate $|U_{+1}|^2$ from Eq. (7), we record two additional images with the DMD in different states. The first image corresponds to a phase shifted representation of the TF of propagation, i.e., $H_{z,\pi} = H_z \exp(i\pi)$, which yields

$$I_{S,\pi} \approx |U_0|^2 + |U_{+1}|^2 - U_0 \cdot U_{+1}^* - U_0^* \cdot U_{+1}. \quad \textbf{(8)}$$

The second image corresponds to a uniform distribution of the DMD, i.e., all mirrors are switched on, so that only the zero-order $I_0 = |U_0|^2$ arises in the sensor plane. With these images, we can finally determine the propagated image I_{+1} to

$$I_{+1} = I_S + I_{S,\pi} - 2 \cdot I_0. \quad \textbf{(9)}$$

Figure 2 shows a photo of the experimental setup. A He–Ne laser ($\lambda = 632.8$ nm) illuminates a rotating diffuser. Thus, the spatial coherence of the light is reduced. The spatially partially coherent light is then used to illuminate the test object. The object is placed at the working distance (WD) of a long distance microscope objective (LDM). The LDM is an object side telecentric microscope objective having a numerical aperture of NA = 0.21 and a WD of 51 mm. Based on Rayleigh criterion, the lateral resolution of the system is 1.8 µm. The image plane of the LDM coincides with the input plane of a $4f$ system, which consists of two identical lenses having a focal length of $f = 150$ mm and a DMD at the common Fourier plane. The DMD is a Texas instrument DLP5500 with 10.8 µm pixel pitch, resolution of 1024 × 768, and a switching rate of up to 5 kHz for binary patterns.

At the front of the DMD, we use a total-internal reflection prism (TI-BS) to adapt the incident and reflected paths of light

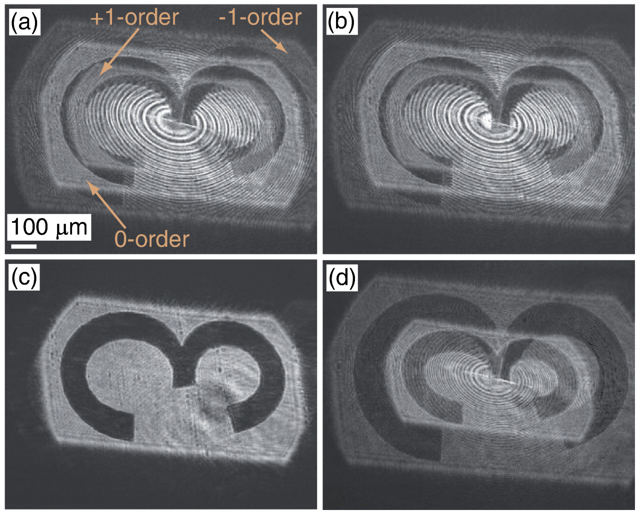

Fig. 3. Experimental results demonstrate the temporal phase shifting scheme that is used digitally to suppress the zeroth order. (a), (b) Images captured for two π shifted $\bar{M}_A$ realizing a propagation of 10 µm at object plane showing the zeroth, +1, and −1 diffraction orders. (c) Image recorded by switching all DMD's micro-mirrors to be on. (d) Result of suppressing the zeroth order. The dynamic range is adapted between zero and one for all images.

towards the DMD and the camera, respectively. At the image plane of the $4f$ system, a high-speed camera (VKTZ Fastcam mini UX 100) with a pixel pitch of 10 µm, and capturing up to 4 kHz at full resolution of 1280 × 1024 pixels, is employed for rapid image recording. Both the camera and the DMD are synchronized during the capturing process. The setup combines the benefit of depth discrimination through partially coherent illumination with the high-speed switching capability of a DMD, to achieve fast depth scan. Consequently, methods based on focus variation microscopy [6] can be applied to determine the object's shape from the recorded intensity measurements.

In the following, we demonstrate the phase shifting approach given by Eq. (9) to eliminate the disturbing contributions of the zeroth order. To achieve this, a TF of propagation is used to achieve a propagation of 10 µm at the object plane. As an object, the number 3 of group 3 of the non-tilted USAF chart (no diffuser attached) is selected. We recorded the intensities I_S and $I_{S,\pi}$, which are shown in Figs. 3(a) and 3(b).

One can see three diffraction orders, i.e., zeroth, +1, and −1 orders, in both images. Additionally, we see interference patterns that correspond to the cross terms in Eq. (6). The +1 order corresponds to the image in focus, whereas the −1 order is the de-focused and darker image. Due to the real valued modulation with M_A, the +1 order has a negative beam of curvature compared with the one resulting from the microscope objective, and thus the +1 order converges and becomes smaller than the zeroth order. On the other hand, the −1 order has the same sign of the beam of curvature as the one resulting from the microscope objective. Thus, the −1-order beam diverges and becomes larger than the zeroth order. The comparably small propagation distance of 10 µm is selected to suit all orders across the field of view of the camera, so that the opposing trend in propagation of the two orders becomes clearly visible. In a real measurement situation, the overall propagation distance is much larger, and the −1 order becomes almost invisible. Figure 3(c) shows the

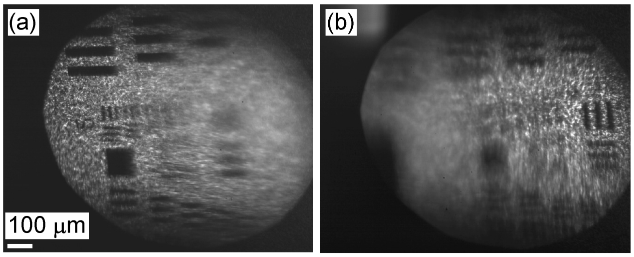

Fig. 4. Experimental results demonstrate the contrast variation across the tilt object during the depth scan from (a) left to (b) right. High contrast appears only for points located at the working distance of the LDM objective. The depth scan process at the whole tilt object is shown in Visualization 1.

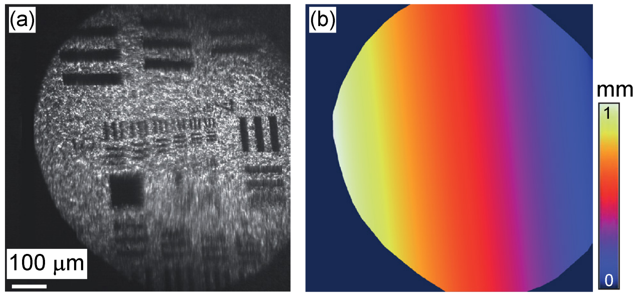

Fig. 5. Results of the (a) reconstructed extended depth image and (b) 3D height map.

image for the case in which all DMD pixels are switched on and represents the zeroth order, except for the overall intensity. Figure 3(d) shows the result corresponding to Eq. (9).

In the following, we measure the form of a test object based on depth discrimination. For this purpose, we attach a fixed diffuser to the USAF chart (USAF + diffuser) and tilt it by an angle of 45° realizing a 3D object with known depth. The test object is adjusted so that its left side (across the field of view) is located at the WD of a 10× magnifying LDM. In consequence, a set of 90 binarized TFs is calculated where 45 of them are un-shifted and the other 45 are π shifted. The step propagation distance within the set is 22.25 µm, thus achieving a depth scan of 1 mm. Please note that, as discussed above, the -1 order becomes larger with increasing the propagation distance, and thus it does not disturb the recorded images since it becomes almost invisible compared with the high-intensity $+1$ order. Inscribing the 90 binarized TFs ($\bar{M}_A$) on the DMD, a set of 90 intensity images in < 25 ms is recorded. These images are used to digitally suppress the zeroth order, resulting in 45 images free from the zeroth order. Figure 4 shows two captured images with a limited depth of focus after suppressing the zeroth-order beam. Visualization 1 shows the complete scan process. As can be seen from the visualization, the images are laterally shifted. This shift has to be compensated for as discussed in Ref. [10] before evaluation.

In analogy to the focus variation approach [6], the Michelson contrast of the images is used as a focus measure to reconstruct the extended depth of focus image shown in Fig. 5(a). For this purpose, the contrast is compared within a window of 16 × 16 pixels for the different depth images to determine a maximum, and the height is defined accordingly. The window is scanned across the whole set of images using the process described above to find the maximum contrast. Using the determination of the local height, i.e., depth of maximum contrast of the intensity, the 3D form of the test object is reconstructed and shown in Fig. 5(b), indicating a maximum depth of ≈1000 µm. Note that areas outside the optics aperture are not defined and set to zero. In order to validate the measured results, we use a simple geometrical consideration given by the fact that the test object is tilted by an angle of 45°. From the captured images, the part of the projection of the object captured by the camera has a diameter of 1008 µm. Due to the tilt of the object, the depth covered by the camera is also 1008 µm, which represents the maximum depth scan of the object. Comparing this result with the reconstructed depth map of ≈1000 µm leads to a maximum difference of around 8 µm. It is noted that for smooth surfaces, the contrast is generally zero, i.e., no features are distinguishable, and thus the proposed approach cannot be used.

In conclusion, we have shown that imaging under spatially partially coherent light can be used for form measurements. The technique uses limited spatially coherent illumination to produce depth discrimination. Thus, images with limited depth of focus are obtained. For fast object scan, a $4f$-imaging system with a DMD located at the common Fourier plane of the two lenses is employed. The DMD is used to manipulate light with binarized TFs of free-space propagation. We achieve a depth scan rate of up to 4 kHz. To compensate for the binarization effect, a temporal phase shifting model is presented. To verify the proposed approach, a tilted USAF test chart with a diffuser attached to it was used as a test object. The contrast of the captured images was implemented as a focus measure to reconstruct an extended depth of focus image that results in the corresponding 3D height map of the test object.

Funding. Deutsche Forschungsgemeinschaft (Project no. 284158589, SPICE).

Disclosures. The authors declare no conflicts of interest.

REFERENCES

1. M. Agour, A. von Freyberg, B. Staar, C. Falldorf, A. Fischer, M. Lütjen, M. Freitag, G. Goch, and R. Bergmann, in *Cold Micro Metal Forming*, F. Vollertsen, B. Kuhfuß, C. Thomy, S. Friedrich, P. Maaß, and H.-W. Zoch, eds. (Springer, 2020), pp. 256–274.
2. U. Schnars and W. Jüptner, Appl. Opt. **33**, 179 (1994).
3. J. C. Wyant, in *Holography: a Tribute to Yuri Denisyuk and Emmett Leith*, Vol. **4737** (International Society for Optics and Photonics, 2002), pp. 98–107.
4. T. Dresel, G. Häusler, and H. Venzke, Appl. Opt. **31**, 919 (1992).
5. M. Agour, C. Falldorf, and R. B. Bergmann, in *Digital Holography and Three-Dimensional Imaging* (Optical Society of America, 2019), pp. W3A–22.
6. F. Helmli, in *Optical Measurement of Surface Topography* (Springer, 2011), pp. 131–166.
7. C. Falldorf, M. Agour, C. V. Kopylow, and R. B. Bergmann, Appl. Opt. **49**, 1826 (2010).
8. C. Falldorf, M. Agour, F. Thiemicke, and R. B. Bergmann, "Lens based phase retrieval under spatially partially coherent illumination - part I: theory," Opt. Laser Eng. (to be published).
9. J. W. Goodman, in *Laser Speckle and Related Phenomena* (Springer, 1975), pp. 9–75.
10. M. Agour, C. Falldorf, C. V. Kopylow, and R. B. Bergmann, Appl. Opt. **50**, 4779 (2011).